




Synthesis, structure, and characterization of two 1-D homometallic coordination polymers based on carboxylate-functionlized salen ligands

Lina Hao, Ying Lu, Zhenzhen He, Qing Lan & Enbo Wang

To cite this article: Lina Hao, Ying Lu, Zhenzhen He, Qing Lan & Enbo Wang (2015) Synthesis, structure, and characterization of two 1-D homometallic coordination polymers based on carboxylate-functionlized salen ligands, Journal of Coordination Chemistry, 68:15, 2682-2690, DOI: 10.1080/00958972.2015.1062093


To link to this article: <http://dx.doi.org/10.1080/00958972.2015.1062093>

 View supplementary material 

 Accepted author version posted online: 16 Jun 2015.
Published online: 09 Jul 2015.

 Submit your article to this journal 

 Article views: 67

 View related articles 

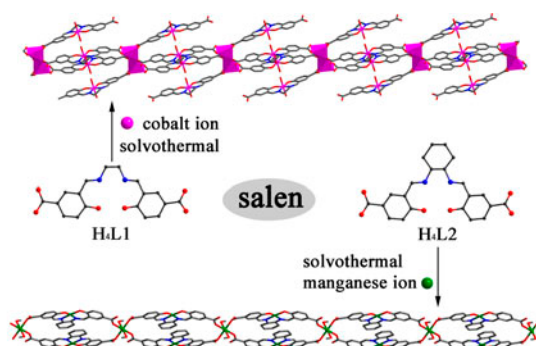
 View Crossmark data 

Synthesis, structure, and characterization of two 1-D homometallic coordination polymers based on carboxylate-functionalized salen ligands

LINA HAO, YING LU*, ZHENZHEN HE, QING LAN and ENBO WANG*

Key Laboratory of Polyoxometalate Science of Ministry of Education, Department of Chemistry, Northeast Normal University, Jilin, PR China

(Received 6 February 2015; accepted 22 May 2015)



Two 1-D homometallic coordination polymers **1** and **2** have been prepared by one-step hydrothermal reactions of carboxylate-functionalized salen ligands with Co(II) and Mn(II), respectively. Single-crystal X-ray diffraction analyses reveal that both the 1-D chains give 3-D supramolecular structures through intermolecular hydrogen bonds and $\pi \cdot \cdot \pi$ packing interactions. Magnetic investigation of **2** indicates the presence of antiferromagnetic interactions in 1-D chains.

Keywords: Salen ligand; Coordination polymer; One-step synthesis; Structure; Magnetic property

1. Introduction

Attention has been devoted to coordination polymers due to their interesting topological structures and many potential applications [1–5]. Selections of metal ions and ligands lead to diverse new structures. Increasing research has focused on the functionalization of ligands for acquiring multifunctional polymeric materials [6–9]. Schiff base ligands bearing two or three donors are of importance due to their simple preparation, diverse structures,

*Corresponding authors. Email: luy968@nenu.edu.cn (Y. Lu); wangeb889@nenu.edu.cn (E. Wang)

and applications in catalysis, biological modeling, and as molecular magnets [10–12]. Tetradentate Schiff base ligands (salen) which can control the reactions and stabilize the spin state of metal center are widely used [13, 14]. As the design and construction of new compounds still play an important role in the study of coordination polymers, salen is considered a vital ligand to fabricate new constructions, especially when additional functional groups are introduced. Among the functional groups, carboxylate-containing ligands are important because of the coordination versatility for tailored design of multifunctional materials [15, 16]. Progress has been achieved in the construction of new compounds with carboxyl-functionalized salen ligands and studies have been made by Cui, Lin and Kitagawa *et al.* [17–21], which dramatically enrich the constructions of higher dimensional heterometallic infinite coordination polymers. The synthetic process of salen-based coordination polymers commonly contains two steps: The first step is the pre-metalation of salen ligand, forming a “metalloligand” (ML) as a precursor; the second step is ML precursor reacts with metal centers to form coordination polymers. We tend to skip synthesis of “metalloligand” and adopt one-step self-assembly of salen ligands and transition metal ions to prepare salen-based coordination polymers. We believe this simplifies the synthetic process for homometallic salen-based coordination polymers. Here, we report two new 1-D coordination polymers **1** and **2** based on dicarboxylate-functionalized salen ligands (H₄L1 and H₄L2) and transition metals (M=Co and Mn). Both compounds are synthesized by one-step synthesis without forming “metalloligand”. Considering Mn-salen coordination polymers have potential applications in magnetic materials [22–24], the magnetic properties of **2** have been studied in this work.

2. Experimental

2.1. Materials and methods

Chemicals were obtained from commercial sources and used without purification. Elemental analyses (C, H, N) were performed on a Perkin–Elmer 2400 CHN elemental analyzer; Co and Mn were determined with a PIASMA-SPEC(I) ICP atomic emission spectrometer in a JEOL JEM 2010-F TEM (200 kV) equipped with a high-resolution pole piece. IR spectra were performed from 400 to 4000 cm⁻¹ using KBr pellets on an Alpha Centaur FT/IR spectrophotometer. Solid-state UV–vis spectra were performed from 200 to 900 nm with a Shimadzu UV-3600 UV–vis spectrophotometer. Thermogravimetric analyses (TGA) were performed with a Perkin–Elmer TG-7 analyzer from room temperature to 600.0 °C at 10 °C min⁻¹ in flowing N₂. Variable temperature magnetic susceptibility was measured at 2–300 K with a MPMS-7SQUID magnetometer.

2.2. Synthesis of H₄L1

3-Formyl-4-hydroxybenzoic acid was obtained by the Reimer–Tiemann reaction [25] of 4-hydroxybenzoic acid with chloroform. A solution of ethylenediamine (0.13 mL, 2 mmol) in 10 mL of ethanol was added dropwise to a solution of 4-formyl-3-hydroxybenzoic acid (0.665 g, 4 mmol) in 20 mL ethanol. The reaction mixture was stirred for 2 h at 60 °C. The resulting yellow solid was filtered and washed with 10 mL cold ethanol and dried *in vacuo* [26].

2.3. Synthesis of H₄L2

The synthetic method of H₄L2 was identical to the preparation of H₄L1 except using *trans*-1,2-diaminocyclohexane (228 mg, 2 mmol) instead of ethylenediamine. The yellow solid was harvested after washing with 10 mL cold ethanol, filtering and drying *in vacuo*.

2.4. Synthesis of [(C₄H₉)₄N]H[PW₁₁Cu(H₂O)₃]

Na₂HPO₄ (1.3 g, 9.1 mmol), Na₂WO₄·2H₂O (33 g, 100 mmol), and Cu(NO₃)₂ (2.88 g, 12 mmol) were dissolved in 200 mL H₂O. The solution was adjusted to pH 4.8 with acetic acid. A solution of TBAB (14.5 g, 45 mmol) in 20 mL H₂O was added dropwise at 80–85 °C. The resulting blue solid was filtered and recrystallized from acetonitrile [27].

2.5. Synthesis of **1**

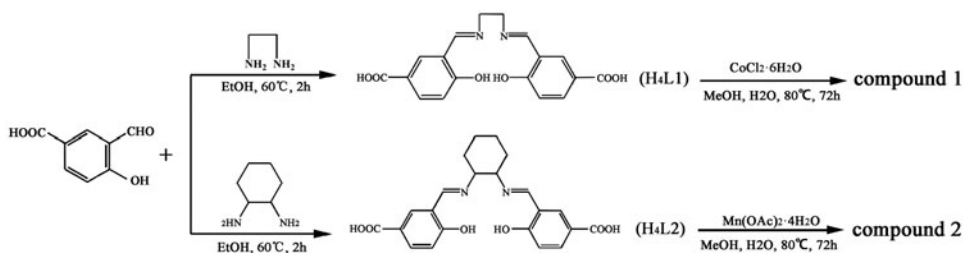
As shown in scheme 1, a solution of CoCl₂·6H₂O (123 mg, 0.5 mmol) in H₂O (10 mL) was added dropwise to a mixture of H₄L1 (90 mg, 0.25 mmol) in MeOH (15 mL). Subsequently [(C₄H₉)₄N]H[PW₁₁Cu(H₂O)₃] (100 mg, 0.033 mmol) was added and stirred for 10 min in air. The mixture was adjusted to pH 8.8 with ammonium hydroxide, then transferred to and sealed in a 15-mL Teflon-lined reactor and heated in an oven to 80 °C for 72 h. The resulting red block crystals of **1** were washed with MeOH, filtered, and dried in air (yield 0.05 g, *ca.* 20%, based on H₄L1). Anal. Calcd (%): C, 43.66; H, 3.64; N, 5.66; Co, 17.89. Found (%): C, 44.33; H, 3.25; N, 6.18; Co, 17.30.

2.6. Synthesis of **2**

The preparation of **2** was similar to **1** except that Mn(OAc)₂·4H₂O (100 mg, 0.4 mmol) was used instead of CoCl₂·6H₂O and H₄L1 was replaced by H₄L2 (100 mg, 0.24 mmol) (scheme 1). Brown block crystals of **2** were obtained after washing with MeOH, filtering, and drying in air (yield 0.02 g, *ca.* 20%, based on H₄L2). Anal. Calcd (%): C, 52.79; H, 4.59; N, 5.36; Mn, 15.78. Found (%): C, 52.03; H, 3.95; N, 6.27; Mn, 16.30.

2.7. X-ray crystallography

X-ray diffraction data were collected with a Bruker AXS SMART 1K CCD diffractometer using graphite-monochromated Mo-K_α radiation at ambient temperature. Data collection



Scheme 1. Syntheses of **1** and **2**.

and reduction were performed using the SMART and SAINT software [28]. A multi-scan absorption correction was applied using SADABS [29]. The structure was solved by direct methods and refined by full-matrix least-squares on F^2 using the SHELXTL program package [30]. Anisotropic thermal parameters were used to refine all non-hydrogen atoms. Hydrogens on carbons were included in calculated positions. Hydrogens on water cannot be found from the weak residual electron peaks but were directly included in the final molecular formula. For **1**, the SQUEEZE program was used to estimate the solvent accessible voids and possible solvent molecules in the structure. Based on the calculation, elemental analysis and TG analysis, another two waters were added directly in the final molecular formula of **1**. The detailed crystal data and structure refinement are given in table S1 (see online supplemental material at <http://dx.doi.org/10.1080/00958972.2015.1062093>). Selected bond lengths and angles of **1** and **2** are listed in tables S2 and S3, respectively.

3. Results and discussion

3.1. Discussion of experimental condition

In a hydrothermal reaction, many factors influence its outcome, including starting concentration, pH, reaction time, and temperature. A series of parallel experiments have been done to find key factors for the formation of **1** and **2**. According to the previous literature, most salen-based coordination polymers were prepared in mixed solvent with DMF or DEF, but the solvents suitable for the isolation of **1** and **2** were the mixed water and methanol. We tried to employ different mixed solvents (MeOH/DMF/H₂O, MeOH/DEF/H₂O, MeOH/DMF, and H₂O/DMF), but no crystal phase was obtained. We also changed the ratio of MeOH and H₂O to optimize the synthetic conditions, coming out with MeOH/H₂O ratio 3:2. The other significant factors are the pH and the introduction of polyoxometalate [(C₄H₉)₄N]H[PW₁₁Cu(H₂O)O₃₉]. Unlike the common pH environment of carboxyl group coordinating to transition metals, **1** and **2** were obtained when the pH was 8.4–9.4. Good crystals suitable for single-crystal determination were obtained at pH 8.8, with no crystal below pH 8.4. The structures of the compounds do not contain the polyoxometalate but no crystallized products could be obtained if we did not add it [31–34]. When temperature and dose ratio were slightly changed, little effect was observed, proving they are less essential factors.

3.2. Crystal structure

Single-crystal X-ray diffraction analysis reveals that **1** adopts a 1-D chain structure (figure 1) and crystallizes in the *P*-1 space group (figure 1). In **1**, there are three crystallographically independent cobalt ions (Co1, Co2, and Co3), all of which have six-coordinate distorted octahedral geometry. Each Co1 is coordinated by four oxygens from two chelate carboxyl groups and two oxygens from two bridging carboxyl groups, while both Co2 and Co3 ions are coordinated by N₂O₂ donors from L1 ligand and two water molecules, forming Co2L1(H₂O)₂ and Co3L1(H₂O)₂ units. The 1-D chain of **1** is constructed by two kinds of units: One is the metalloligand CoL1(H₂O)₂ unit and the other is the dinuclear cobalt unit. CoL1(H₂O)₂ units adopt two distinct types to connect with Co₂, Co2L1(H₂O)₂ uses one chelate carboxyl group to link with one Co₂ unit, while Co3L1(H₂O)₂ uses one chelate carboxyl

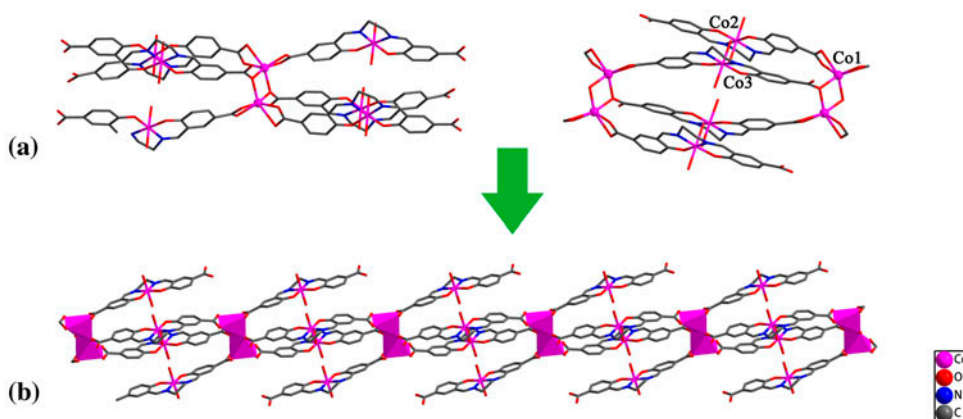


Figure 1. (a) The local connections between dinuclear cobalt units and H_4L_1 in **1** and (b) 1-D chain of **1**.

group and one bridging carboxyl oxygen to connect with two Co_2 units, respectively. The valence sum calculations on the cobalt sites indicate that Co_1 is +2 and both Co_2 and Co_3 are +3 oxidation state. The O/H unit of the coordinated H_2O molecules forms a hydrogen bond to one oxygen from a chelate carboxylate group with $O02 \cdots H \cdots O15 = 2.880(3) \text{ \AA}$, indicating strong hydrogen bonding interactions. The hydrogen bonding interactions facilitate formation of a further 2-D network. The $\pi \cdots \pi$ interactions between layers drive the 2-D network into a 3-D supramolecular structure as shown in figure S1.

Single-crystal X-ray diffraction reveals that **2** adopts a 1-D chain structure [figure 2(a)] and crystallizes in the $P-1$ space group. In **2**, there are two distinct Mn coordination environments, one (Mn1) is located in the center of the salen ligand and is coordinated in a distorted square-planar geometry with two nitrogens and two oxygens from L2 to form a metalloligand MnL, while the other (Mn2) exhibits a distorted octahedral geometry defined

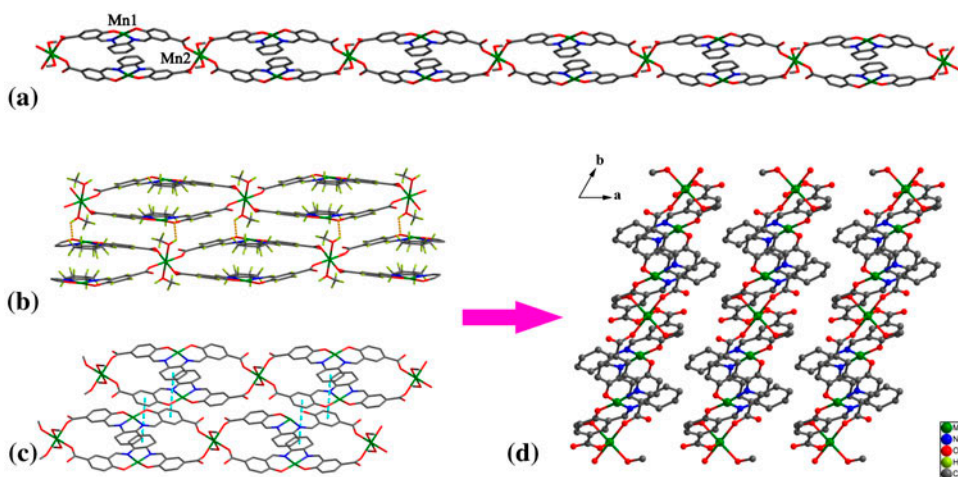


Figure 2. (a) 1-D Chain of **2**, (b) 2-D sheet assembled via intermolecular hydrogen bond, and (c) $\pi \cdots \pi$ packing interactions, and (d) 3-D supramolecular structure in the ab plane.

by four oxygens from four distinct monodentate carboxyl groups and two oxygens from two methanol molecules. The valence sum calculations indicate that Mn1 is in the +3 oxidation state, and Mn2 in +2 oxidation state. Adjacent Mn2 centers are connected by double MnL linkers to form a 1-D chain in **2**. There exists hydrogen bonding interactions between the O\H unit of the coordinated CH₃OH and one oxygen of the N₂O₂ unit which facilitates formation of a further 2-D staggered layer [35–37]. 2-D layers are connected into a 3-D supramolecular structure through interchain $\pi \cdots \pi$ packing interactions involving hexamethylene and aromatic rings (figure 2).

There are only three examples of 1-D chains built by M-salen ligands and transition metal ions. Huang *et al.* reported a 1-D homochiral nickel coordination polymer constructed by enantiopure pyridyl-functionalized salen(Ni) units, 4,4'-biphenyldicarboxylic acids, and Ni ions [38]. Mirkin *et al.* prepared a 1-D homochiral coordination polymer based on Cu-salen units and Cu ions [39]. Cui *et al.* reported a zigzag chain structure formed by self-assembly of Zn-salen units [40]. Compounds **1** and **2** provide two new structure types for the 1-D chains built by M-salen ligands and transition metal ions.

3.3. FT-IR spectroscopy

IR spectra of **1** and **2** are shown in figure S2. The peaks at 1600 cm⁻¹ in **1** and **2** are attributed to $\nu(\text{C}=\text{N})$, which red-shift. The weak intensity and band movement of C=N vibration suggest coordination of azomethine. The peak at 1275 cm⁻¹ is assigned to the –Ph–O asymmetric stretch vibration. Absorption bands in both **1** and **2** at 400–600 cm⁻¹ are attributed to formation of M–O and M–N bonds [41–43].

3.4. UV–vis spectroscopy

The solid-state UV–vis spectra of **1** and **2** are similar (figure S3) and are in complete agreement with the coordination environment as revealed by X-ray single-crystal structure analysis. They both present obvious peaks at 220 nm for **1** and at 218 nm for **2** that can be attributed to $\pi\text{--}\pi^*$ transitions of the aromatic ring and conjugated systems of the ligand. Bands at 349 nm for **1** and 333 nm for **2** are most likely due to $\pi\text{--}\pi^*$ transfer in C=N [44]. As for most salen coordination polymers, there also exists broad absorption bands at 400–500 nm, 497 nm for **1** and 489 nm for **2**, which are characteristic of the coordination sphere between transition metal and N₂O₂ unit in salen [45].

3.5. Thermogravimetric analyses

Both **1** and **2** are stable at room temperature for a couple of months. TGA measurements were performed for **1** and **2** from room temperature to 600 °C (figure S4). The result for **1** reveals three weight loss steps, with experimental mass losses matched well to the calculated. The first weight loss is 9.25% (Calcd 10.92%) from 26 to 156 °C, corresponding to the removal of coordinated and lattice water molecules. At higher temperature, two continuous weight losses are observed from 203 to 434 °C, which are attributed to decomposition of the organic components (observed 68.18%, Calcd 66.34%). The TGA of **2** reveals that two coordinated methanol molecules are lost at 121–172 °C (observed 7.74%, Calcd 6.12%). Then, the compound remained stable until the appearance of continuous weight losses from 267 to 428 °C, which indicates that the crystal structure collapses (observed 71.31%, Calcd 71.21%).

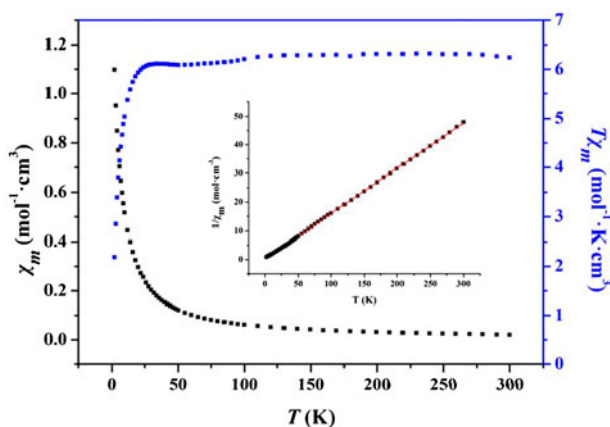


Figure 3. Temperature dependence of $\chi_m T$ values for **2**; (inset) temperature dependence of reciprocal magnetic susceptibility χ_m^{-1} .

3.6. Magnetic property of **2**

The variable temperature magnetic susceptibility data for **2** were collected from 2 to 300 K (figure 3). The $\chi_m T$ value for **2** at 300 K is $6.20 \text{ mol}^{-1} \text{ K cm}^3$, lower than the theoretical value of $10.39 \text{ mol}^{-1} \text{ K cm}^3$ corresponding to the sum of the contributions of the three manganese ions (Mn(II): $S = 5/2$, $g = 2$; Mn(III): $S = 2$, $g = 2$). By decreasing the temperature, $\chi_m T$ almost remains constant in the high-temperature region. On further cooling, $\chi_m T$ begins to decrease sharply at 30.34 K, reaching a minimum at 2.17 K of $2.19 \text{ mol}^{-1} \text{ K cm}^3$. The decrease of $\chi_m T$ in the low-temperature region may be due to zero-field splitting of the ground state of M(III) and/or the interdimer antiferromagnetic interactions [46–48]. The inverse susceptibility plot as a function of temperature is linear above 50 K by the Curie–Weiss law, $\chi_m = C/(T - \theta)$ with the Weiss constant, $\theta = -2.09 \text{ K}$ and the Curie constant, $C = 6.35 \text{ mol}^{-1} \text{ K cm}^3$. The negative Weiss constant and the decrease of $\chi_m T$ with the temperature denote an antiferromagnetic coupling in **2**.

4. Conclusion

Two new salen-based coordination polymers with 1-D chain structures have been isolated. The preparation of **1** and **2** suggests one-step synthesis is feasible in getting homometallic salen-based coordination polymers, which will open up a promising approach to obtain new salen-based materials. Meanwhile, the antiferromagnetic coupling in **2** is a supplement for salen-type magnetic materials.

Supplementary materials

Crystallographic data for the structural analysis has been deposited with the bridge Crystallographic Data Center, CCDC reference number 1046121 for **1** and 1046123 for **2**. These data can be obtained free of charge from the Cambridge Crystallographic Data Center via www.ccdc.cam.ac.uk/data_request/cif.

Disclosure statement

No potential conflict of interest was reported by the authors.

Funding

This work was financially supported by the National Natural Science Foundation of China [grant number 20901015]; Science and Technology Development Project Foundation of Jilin Province [grant number 20130101006JC]; National Grand Fundamental Research 973 Program of China [grant number 2010CB635114].

References

- [1] J.S. Seo, D. Whang, H. Lee, S.I. Jun, J. Oh, Y.J. Jeon, K. Kim. *Nature*, **404**, 982 (2000).
- [2] O.M. Yaghi, M. O'Keeffe, N.W. Ockwig, H.K. Chae, M. Eddaoudi, J. Kim. *Nature*, **423**, 705 (2003).
- [3] M. Oh, C.A. Mirkin. *Nature*, **438**, 651 (2005).
- [4] A.M. Spokoyny, D. Kim, A. Sumrein, C.A. Mirkin. *Chem. Soc. Rev.*, **38**, 1218 (2009).
- [5] D.J. Tranchemontagne, J.L. Mendoza-Cortés, M. O'Keeffe, O.M. Yaghi. *Chem. Soc. Rev.*, **38**, 1257 (2009).
- [6] D. Bradshaw, J.E. Warren, M.J. Rosseinsky. *Science*, **315**, 977 (2007).
- [7] Z. Lin, J. Lü, M. Hong, R. Cao. *Chem. Soc. Rev.*, **43**, 5867 (2014).
- [8] X. Wang, J. Luan, H. Lin, C. Xu, G. Liu, J. Zhang, A. Tian. *Cryst. Eng. Commun.*, **15**, 9995 (2013).
- [9] Y. Li, H. Lun, C. Xiao, Y. Xu, L. Wu, J. Yang, J. Niu, S. Xiang. *Chem. Commun.*, **50**, 8558 (2014).
- [10] T. Takeuchi, A. Böttcher, C.M. Quezada, M.I. Simon, T.J. Meade, H.B. Gray. *J. Am. Chem. Soc.*, **120**, 8555 (1998).
- [11] T. Takeuchi, A. Böttcher, C.M. Quezada, T.J. Meade, H.B. Gray. *Bioorg. Med. Chem.*, **7**, 815 (1999).
- [12] H. Yang, L. Zhang, L. Zhong, Q. Yang, C. Li. *Angew. Chem. Int. Ed.*, **46**, 6861 (2007).
- [13] J.M. Ready, E.N. Jacobsen. *Angew. Chem. Int. Ed.*, **41**, 1374 (2002).
- [14] P.G. Cozzi. *Angew. Chem. Int. Ed.*, **42**, 2895 (2003).
- [15] H. Miyasaka, K. Mizushima, S. Furukawa, K. Sugiura, T. Ishii, M. Yamashita. *Cryst. Liq. Cryst. Sci. Technol., Sect. A*, **379**, 171 (2002).
- [16] J. Heo, Y.M. Jeon, C.A. Mirkin. *J. Am. Chem. Soc.*, **129**, 7712 (2007).
- [17] R. Kitaura, G. Onoyama, H. Sakamoto, R. Matsuda, S. Noro, S. Kitagawa. *Angew. Chem. Int. Ed.*, **43**, 2684 (2004).
- [18] F. Song, C. Wang, J.M. Falkowski, L. Ma, W. Lin. *J. Am. Chem. Soc.*, **132**, 15390 (2010).
- [19] C. Zhu, G. Yuan, X. Chen, Z. Yang, Y. Cui. *J. Am. Chem. Soc.*, **134**, 8058 (2012).
- [20] C. Zhu, X. Chen, Z. Yang, X. Du, Y. Liu, Y. Cui. *Chem. Commun.*, **49**, 7120 (2013).
- [21] G. Yuan, C. Zhu, Y. Liu, Y. Cui. *Chem. Commun.*, **47**, 3180 (2011).
- [22] D. Gatteschi, R. Sessoli. *Angew. Chem. Int. Ed.*, **42**, 268 (2003).
- [23] S.K. Ritter. *Chem. Eng. News*, **82**, 28 (2004).
- [24] A.J. Tasiopoulos, A. Vinslava, W. Wernsdorfer, K.A. Abboud, G. Christou. *Angew. Chem. Int. Ed.*, **43**, 2043 (2004).
- [25] H. Wynberg. *J. Am. Chem. Soc.*, **76**, 4998 (1954).
- [26] A. Bhunia, P.W. Roesky, Y. Lan, G.E. Kostakis, A.K. Powell. *Inorg. Chem.*, **48**, 10483 (2009).
- [27] C.M. Tourné, G.F. Tourné, S.A. Malik, T.J.R. Weakley. *J. Inorg. Nucl. Chem.*, **32**, 3875 (1970).
- [28] G.M. Sheldrick. *SADABS Program for Scaling and Correction of Area Detector Data*, University of Göttingen, Göttingen (1996).
- [29] Bruker. *APEXII software, (Version 6.3.1)*, Bruker AXS Inc., Madison, WI (2004).
- [30] G.M. Sheldrick. *SHELXL-97, Program for X-ray Crystal Structure Refinement*, University of Göttingen, Göttingen (1997).
- [31] R. Tsunashima, D. Long, H.-N. Miras, D. Gabb, C.-P. Pradeep, L. Cronin. *Angew. Chem. Int. Ed.*, **49**, 113 (2010).
- [32] J. Niu, F. Li, J. Zhao, P. Ma, D. Zhang, B. Bassil, U. Kortz, J. Wang. *Chem. Eur. J.*, **20**, 9852 (2014).
- [33] P. Huang, C. Qin, Z. Su, Y. Xing, X. Wang, K. Shao, Y. Lan, E. Wang. *J. Am. Chem. Soc.*, **134**, 14004 (2012).
- [34] J. Niu, G. Wang, J. Zhao, Y. Sui, P. Ma. *J. Wang. Cryst. Growth Des.*, **11**, 1253 (2011).
- [35] I. Nemeč, R. Herchel, T. Šilha, Z. Trávníček. *Dalton Trans.*, **43**, 15602 (2014).
- [36] T. Wang, M. Ren, S. Bao, Z. Cai, B. Liu, Z. Zheng, Z. Xu, L. Zheng. *Dalton Trans.*, **44**, 4271 (2015).
- [37] M.A. Siegler, M. Lutz. *Cryst. Growth Des.*, **9**, 1194 (2009).
- [38] Y. Huang, T. Liu, J. Lin, J. Lü, Z. Lin, R. Cao. *Inorg. Chem.*, **50**, 2191 (2011).
- [39] J. Heo, Y. Jeon, C.A. Mirkin. *J. Am. Chem. Soc.*, **129**, 7712 (2007).
- [40] G. Li, C. Zhu, X. Xi, Y. Cui. *Chem. Commun.*, **45**, 2118 (2009).

- [41] T. Kurahashi, H. Fujii. *Inorg. Chem.*, **52**, 3908 (2013).
- [42] C. Yuan, X. Yang. *Inorg. Chem. Commun.*, **48**, 57 (2014).
- [43] C. Zhu, F. Ban, E. Sheng, S. Zheng, B. Liu, Y. Cui. *Chin. J. Struct. Chem.*, **32**, 205 (2013).
- [44] T. Ghosh, B. Mondal, T. Ghosh, M. Sutradhar, G. Mukherjee, M.G.B. Drew. *Inorg. Chim. Acta*, **360**, 1753 (2007).
- [45] S. Akine, T. Taniguchi, T. Nabeshima. *Chem. Lett.*, **30**, 682 (2001).
- [46] M. Kurmoo. *Chem. Soc. Rev.*, **38**, 1353 (2009).
- [47] Y. Li, W. Zou, M. Wu, J. Lin, F. Zheng, Z. Liu, S. Wang, G. Guo, J. Huang. *Cryst. Eng. Commun.*, **13**, 3868 (2011).
- [48] M. Zhang, W. Shan, Z. Han. *Cryst. Eng. Commun.*, **14**, 1568 (2012).